

Observational evidence for the link between the compact jet and optical continuum in the radio galaxy 3C 390.3

T.G. Arshakian¹, A.P. Lobanov¹, V.H. Chavushyan², A.I. Shapovalova³, J.A. Zensus¹

¹ MPIfR (tigar@mpifr-bonn.mpg.de), ² INAOE & IA-UNAM, ³ SAO RAS



Summary

The “central engine” of AGN is thought to be powered by accretion on a central nucleus believed to be a super-massive black hole. The localization and exact mechanism of the energy release in AGN are still not well understood. We present observational evidence for the link between variability of the radio emission of the compact jet, optical and X-ray continua emission and ejections of new jet components in the radio galaxy 3C 390.3. These correlations indicate that the source of variable non-thermal continuum radiation is located in the innermost part of the relativistic jet. We suggest that the continuum emission from the jet and counterjet ionizes material in a subrelativistic outflow surrounding the jet, which results in a formation of two conical regions with broad emission lines (in addition to the conventional broad line region around the central nucleus) at a distance more than or equal to 0.4 parsecs from the central engine.

To search for a relation between variability of the optical continuum flux and changes in the radio structure of the radio-loud broad emission-line galaxy 3C 390.3 ($z=0.0561$) on scales of ~ 1 pc, we combine the data from monitoring in the optical, UV, and X-ray regimes with very long baseline interferometry (VLBI) observations of its radio emission at 15 GHz made from 1992 to 2002 using the VLBA (Very Long Baseline Array).

Structure and kinematics of the pc-scale jet

Using 10 epochs of VLBI measurements, we identified five moving components C4–C8 (in addition to the previously known components C2 and C3) and two stationary features S1 and S2 separated from D by 0.28 ± 0.03 mas and 1.50 ± 0.12 mas (1 mas ≈ 1.09 pc, Fig. 1). Linear fits to the observed separations of the component C4–C8 from the component D yield proper motions of $0.2\text{--}0.4$ mas/yr, which correspond to apparent speeds of $0.8\text{--}1.5c$. We used the linear fits to estimate, for each moving component, the epoch, t_D , at which it was ejected from the component D and the epoch, t_{S1} , when it passed through the location of the stationary feature S1 (Fig. 1, right panel).

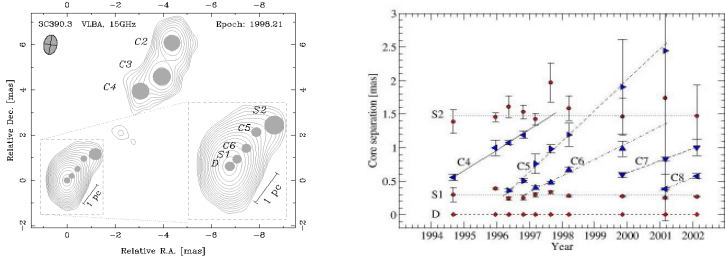


Figure 1. Left panel: Radio structure of 3C 390.3 observed in 1998.21 with VLBI at 15 GHz (2 cm). Innermost fraction of the jet is shown in the inset. Right panel: Separation of the jet components relative to the stationary feature D (diamonds) for ten epochs of VLBI observations. Moving components are denoted by leftward triangles (C4), rightward triangles (C5), upward triangles (C6), downward triangles (C7), leftward triangles (C8), and stationary components S1 and S2 are marked by circles. The lines represent the best linear least-squares fits to the component separations.

Correlations between the jet and optical continuum emission

In Fig. 2, the properties of the components D and S1 identified in the radio jet are compared with the optical continuum emission at 5100Å and 1850Å.

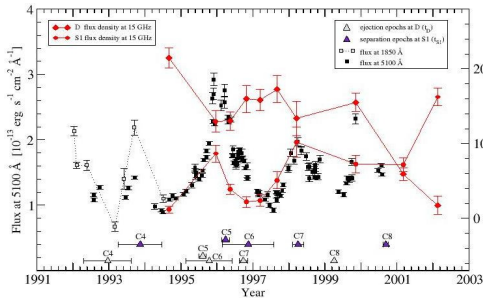


Figure 2. The variations of the continuum fluxes of 3C 390.3 during the 1992 to 2002.2 time period. Optical continuum light curve at 5100Å (Shapovalova et al. 2000; Sergeev et al. 2001) (black squares), UV continuum fluxes (Zheng 1996) scaled by a factor of 50 (grey squares), and variations of radio flux density from D and S1 components (filled red diamonds and circles) are presented. The times of ejection, t_D , of radio knots from D (presumed base of the jet) and the times of their separation, t_{S1} , from the component S1 are marked by open triangles and filled triangles respectively.

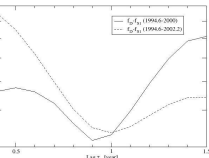
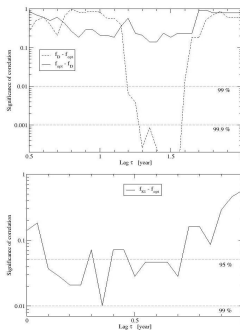


Figure 3. The normalized χ^2 statistic as a function of time delay between radio light-curves of D and S1 components. Each radio light curve is linearly interpolated, and the data points of one light curve is shifted. For every shift we calculate the normalized $\chi^2(N-n)$, where N is the number of overlapped points and $n=2$ is the number of fitted parameters.



The time delay between variations of f_D and optical continuum flux (f_{opt}) is determined using the Spearman's rank correlation coefficient (Fig. 4, top panel). This method has been applied to the optical (106 points) and radio (eight points) data measured between 1992 and 2002. A significant correlation ($>99\%$, see Fig. 4) is present between f_D and f_{opt} for time lags ranging from $\sim(1.2\text{--}1.6)$ yr. No significant correlation is found in the $f_{opt}\text{--}f_D$ relation plane where the optical continuum is assumed to lead the radio emission. This result strongly suggests that:

- The radio emission precedes the optical continuum by ~ 1.4 yr.
- There should be a physical relation between variable radio emission from the feature D of the jet and optical continuum emission.

Figure 4. Top panel: The probability of the Spearman's rank correlation coefficient for different time delays between f_D and f_{opt} (dashed line) and f_D and f_{1850} (solid line) light curves. The horizontal dotted lines corresponds to the 99% and 99.9% confidence levels. Bottom panel: The probability as a function of time delay between f_{1850} and f_{opt} light curves.

The time delay between variations of f_{S1} and f_{opt}

One should expect that the optical continuum also correlates with and follows the radio emission of S1 component with time delay of $t_{S1,opt} = t_{D,opt} - t_{D,S1} \sim 0.4$ yr. Fig. 4 (bottom panel) shows that there is a positive correlation (at the $\geq 95\%$ confidence level) in the $f_{S1} - f_{opt}$ relation plane for a wide range of time lags from ~ 0 yr to ~ 0.7 yr. It is most probable that the optical continuum is produced near or at the location of the radio emission (0–0.4 light year from the feature S1).

Supporting evidence for the link between S1 component of the jet and optical continuum

For the components C4–C7, the epochs S1 of separation from the stationary feature S1 are coincident, within the errors, with the maxima in the optical continuum (Fig. 2). All four ejection events occur within ~ 0.3 yr after a local maximum is reached in the intensity of the optical continuum (the average time delay between the maxima and the epochs t_{S1} is 0.18 ± 0.06 years). The null hypothesis that this happens by chance is rejected at a confidence level of 99.98%.

The central pc-scale region in the 3C 390.3

D component: The link between the radio emission from D and S1 suggests that the appearance of these stationary features in the jet is due to physical, rather than geometrical, factors. The component D is likely to be the proverbial “base” of the VLBI jet near the central engine (Fig. 6); the base being the location at which the flow either becomes supersonic or optically thin or releases the energy contained in the Poynting Flux. The identification of the component D with the central engine is supported by the correlation between the ejection epoch, t_D , of the component C5 and the variability of the X-ray flux at 0.1–2 keV (Fig. 5). The ejection of C5 occurred after a dip in the X-ray emission and hardening of the spectrum suggesting (similar to 3C 120; Marscher et al. 2002) that the soft X-ray emitting disk material disappears into the black hole and a fraction of the infalling matter is ejected into the jet.

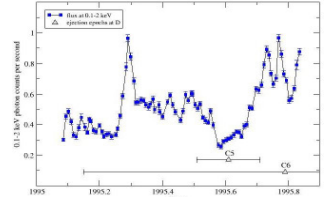


Figure 5. The variations of soft X-ray fluxes at 0.1–2 keV (Liegthy et al. 1997) for 3C 390.3 between 1995 and 1996 superimposed with the epochs of origin of C5 and C6. 1 σ error bars are presented for all data.

S1 component then can be associated with the stationary radio feature which may be produced by the internal oblique shock formed in the continuous relativistic flow (Gomez et al. 1995). In this scenario, the energy release in the form of variable radiation can be produced by interaction of relativistically moving compact component (shock?) with the stationary shocks produced at the positions of D and S1 of the jet. In this scenario, the time delay between variations of f_D and f_{S1} is equal to the time ($t_{D,S1} = t_{D,S1}$) at which the ejected component passes from D to S1. This is in fact the case for the 3C 390.3 (1 yr ~ 1.04 yr). The characteristics of a long-term variability of optical continuum flux are likely to be related to the properties of the jet such as the jet ejection rate, structure and kinematics of the sub-parsec scale jet.

Optical continuum emission.

Location. The bulk of variable continuum is generated in the innermost part of the jet at a large distance (≥ 0.4 pc) from the central engine (Fig. 6).

Size. The region from which the optical continuum is emitted should be ~ 5 light days inferred from the time delay of about 5 days between variations of the optical flux at 5100 Å and the UV and soft X-ray emission (Dietrich et al. 1998).

Emission mechanism. The variable continuum emission is of non-thermal origin which is supported by:

- a link between optical continuum and radio synchrotron emission of the jet, and,
- a single power-law ($\alpha=0.89$) for a spectral range from optical to soft X-ray (Dietrich et al. 1998).

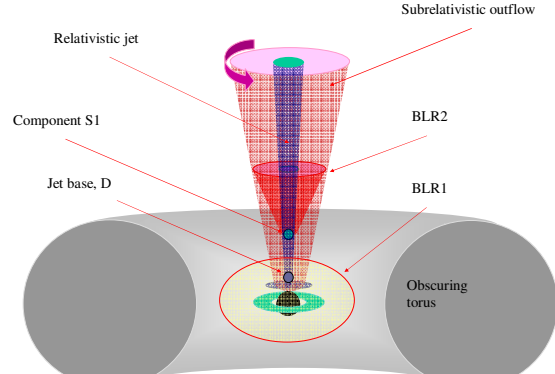
Broad-line region (BLR)

The optical continuum emission of 3C 390.3 leads the double-peaked H β line emission by $\sim(30\text{--}100)$ days (Shapovalova et al. 2000). The localization of the source of opt. continuum with the innermost part of the jet suggests that there are two different BLRs (Fig. 6):

- The BLR2 is ionized by continuum emission of the jet in the rotating subrelativistic outflow surrounding the jet. The BLR2 is evident in the broad-line emission at times when the jet emission dominates the opt. continuum (see Fig. 2).
- The BLR1 is associated with the central nucleus and can be hidden (partially?) from the observer. The BLR1 may be manifested in the broad-line emission around the epochs of minima in the continuum flux, when the jet contribution to the ionizing continuum is small.

The conical form of BLR2 arises from a large fraction of the continuum radiation being beamed into a cone with a half-opening angle $\sim 30^\circ$. The double-peaked structure of the H β line can be reproduced in the BLR2 by a rotation of the approaching jet and a subrelativistic outflow (Murray et al. 97; Proga et al. 2000).

Figure 6. A sketch of the nuclear region in 3C 390.3



Challenges

- The large distance of the BLR2 from the central engine (~ 0.4 pc) challenges the existing models in which the broad-line emission is localized exclusively around the disk or near the central engine.
- It also questions the assumption of virialized motion in the BLR of radio-loud galaxies, which forms the foundation of the method for estimating black hole masses from reverberation mapping (Peterson 2002).

Predictions

- The model (Fig. 6) suggests that there should be two BLR2s: (1) one associated with the jet and (2) one associated with the counterjet. The optical/UV/X-ray line emissions from BLR2 in the counterjet are free from relativistic effects and have better chances to penetrate the absorbing medium towards the observer. Detection of a time lag between correlated variability of emission lines from the far-side and near-side BLR2s would be the most direct observational evidence for double BLRs ionized by the continuum radiation from the bases of the jet and counterjet. A time delay of ~ 2 years is expected for such variations in 3C 390.3.
- The rotating and approaching BLR2 will imprint prominent signatures on the emission lines. Depending on the orientation of the jet the BLR2 may produce non-blue-shifted and single/double-peaked emission lines.